The hydration of aniline: Analysis of spatial distribution functions

Andriy Plugatyr and Igor M. Svishchev

Citation: The Journal of Chemical Physics **130**, 114509 (2009); doi: 10.1063/1.3096672
View online: http://dx.doi.org/10.1063/1.3096672
View Table of Contents: http://scitation.aip.org/content/aip/journal/jcp/130/11?ver=pdfcov
Published by the AIP Publishing

The hydration of aniline: Analysis of spatial distribution functions

Andriy Plugatyr and Igor M. Svishchev[a)]
Department of Chemistry, Trent University, Peterborough, Ontario K9J 7B8, Canada

(Received 16 December 2008; accepted 18 February 2009; published online 20 March 2009)

Molecular dynamics simulations of aniline in aqueous infinitely dilute solution are performed from ambient to supercritical conditions. Spatial hydration structures of aniline are examined along the liquid branch of the liquid-vapor coexistence curve of the simple point charge/extended water model at 298, 373, 473, and 573 K and in the supercritical region at 633, 733, and 833 K with density fixed at 0.3 g/cm^3. The coordination and H-bond numbers of aniline are calculated. The self-diffusion coefficient of aniline is also evaluated. At room temperature the solvation shell of aniline is comprised of ~32 water molecules. At 298 K, the amino group is hydrated by three water molecules with which it forms one strong and two weak (0.6) H bonds acting as an acceptor and donor, respectively. In addition, ~1.5 water molecules are identified as π-coordinated, forming close to 0.75 H bonds with the aromatic ring of aniline. The features of the hydration shell structure of aniline diminish with temperature and decreasing density. The disappearance of π-coordinated water molecules is noted at around 473 K, whereas the loss of the hydrophobic solvent cage is observed near the critical point of water. At supercritical conditions aniline is hydrated by approximately eight water molecules with the amino group coordinated to roughly two of them, forming less than one H bond in total. © *2009 American Institute of Physics*. [DOI: 10.1063/1.3096672]

I. INTRODUCTION

Over the past two decades, near-critical water has attracted much attention as a promising medium for a variety of technological applications such as power generation, hazardous waste utilization, materials processing, etc.[1–6] The development and optimization of these technologies require thorough examination of complex properties of near-critical aqueous solutions. Understanding the effect of *solvent* on the diffusivity and reactivity of *solutes* at sub- and supercritical water conditions is of particular interest. The loss of the extended H-bonded structure of water at near-critical conditions enhances the diffusivity of solutes. On the other hand, the disappearance of the solvent "cage" affects the reaction kinetics as the number of collisions per encounter decreases from "multiple" at ambient conditions to a "single" event in a low-density supercritical water. The interplay between these two factors is particularly pronounced for rates of near-diffusion-controlled reactions that exhibit non-Arrhenius behavior (with negative temperature dependence) in the range of about 423–623 K.[7–15] Systematic studies on molecular dynamics (MD) and hydration structures are clearly warranted to provide a detailed understanding of the chemical reaction mechanisms in water at near-critical conditions.

From a chemical perspective, the information about mass transport coefficients and hydration structures of the reacting species is essential for estimation of the diffusion-controlled limit via the Smoluchowski equation. Unfortunately, very little is known about the diffusivity of organic solutes at near and above the critical point of water.[16–19] Furthermore, the simple hydrodynamic (Stokes–Einstein–Debye) approach, commonly used for the calculation of the mass transport coefficients at ambient conditions, does not adequately describe the behavior of the self-diffusion coefficient of water at near and above its critical point.[20,21]

In this study we examine the solvation structures and self-diffusion coefficients of aniline in aqueous infinitely dilute solution from ambient to supercritical conditions. Aniline is an important model system which allows for the study of both hydrophilic and hydrophobic hydration. Small gas-phase aniline-water complexes have been previously examined by several research groups.[22–24] Spoerel and Stahl[22] and Piani *et al.*[24] studied the properties of the 1:1 aniline-water complex. The results indicate that in this complex water is H bonded to aniline with the interaction taking place at the lone pair of the nitrogen. Inokuchi *et al.*[23] studied the infrared photodissociation spectra of $[\text{aniline-(H2O)}_n]^+$ ($n=1-8$) complexes which were interpreted with the aid of density functional theory calculations. The authors show that for $n=2$, water forms 1-1 H-bonded structure with each amino hydrogen of aniline, whereas for $n=3$, a 2-1 branched complex was reported.

A number of computer simulation studies, focused on the properties of aqueous amine solutions,[25–32] indicate that at ambient conditions the amino group is coordinated by about three water molecules and exhibits much better H-bond accepting than H-bond donating character.[25,27,29–31]

The goal of this study is to examine the hydration structure and diffusivity of aniline from ambient to supercritical water conditions. The remainder of the paper is organized as

[a)]Author to whom correspondence should be addressed. FAX: 1-705-748-1625. Electronic mail: isvishchev@trentu.ca.

TABLE I. Electrostatic, geometric, and LJ parameters for water and aniline models.

Species	Atom	ε (kcal/mol)	σ (Å)	q (e)	$\boldsymbol{R}$ (Å)	∥ (deg)
H_2O[a]	H	0.0000	0.0000	0.4238		109.47 (H–O–H)
	O	0.1554	3.1660	−0.8476	1.000	
$C_6H_5NH_2$[b]	C_{ipso}	0.070	3.550	0.180	1.400 (C=C)	120.0 (CCC)
	C_A	0.070	3.550	−0.115	1.080 (C–H)	120.0 (CCH)
	H_A	0.030	2.420	0.115	1.430 (C–N)	120.0 (CCN)
	N	0.170	3.300	−0.900	1.010 (N–H)	111.0 (CNH)
	H(N)	0.000	0.000	0.360		106.4 (HNH)

[a]Reference 33.
[b]Reference 29.

follows. Computational details are described in Sec. II. Simulation results are discussed in Sec. III. Our conclusions are given in Sec. IV.

II. SIMULATION DETAILS

In this study the simple point charge extended (SPC/E) (Ref. 33) water model was used. The SPC/E model is a very attractive pair potential for the study of aqueous solutions over a wide range of states from ambient to supercritical conditions as it captures reasonably well (within limitations of the rigid point charge potential) experimental properties of real water, see Refs. 34–39 and therein. Phase coexistence studies, performed so far, indicate that the SPC/E potential provides a good description of the liquid-vapor coexistence properties of water.[34,37–41] Note that the results for the exact location of the critical point of the SPC/E water somewhat disagree but fall within temperature and density ranges of 630–641 K and 0.26–0.31 g/cm^3, respectively.

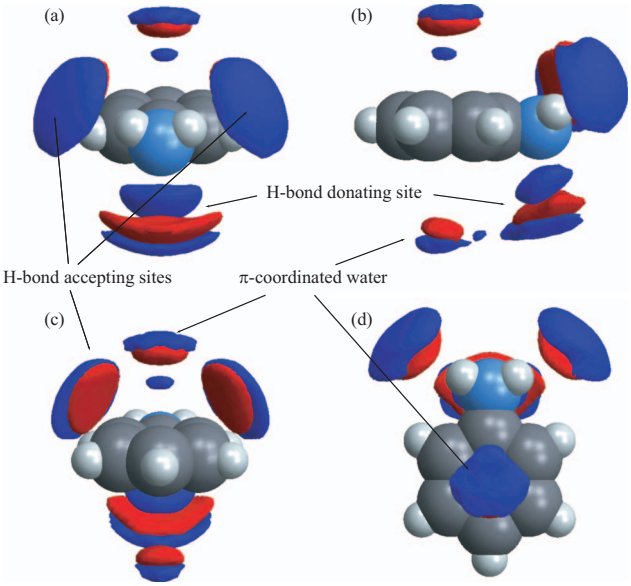

FIG. 1. (Color) The SDF of water around central aniline molecule at 298 K. Local atomic densities of oxygen (red) and hydrogen (blue) of water are shown at probability levels of $\boldsymbol{G}_O(r,\boldsymbol{\Omega})=2.5$ and $\boldsymbol{G}_H(r,\boldsymbol{\Omega})=1.8$, respectively. (a) Front view; (b) side view; (c) rear view; and (d) top view.

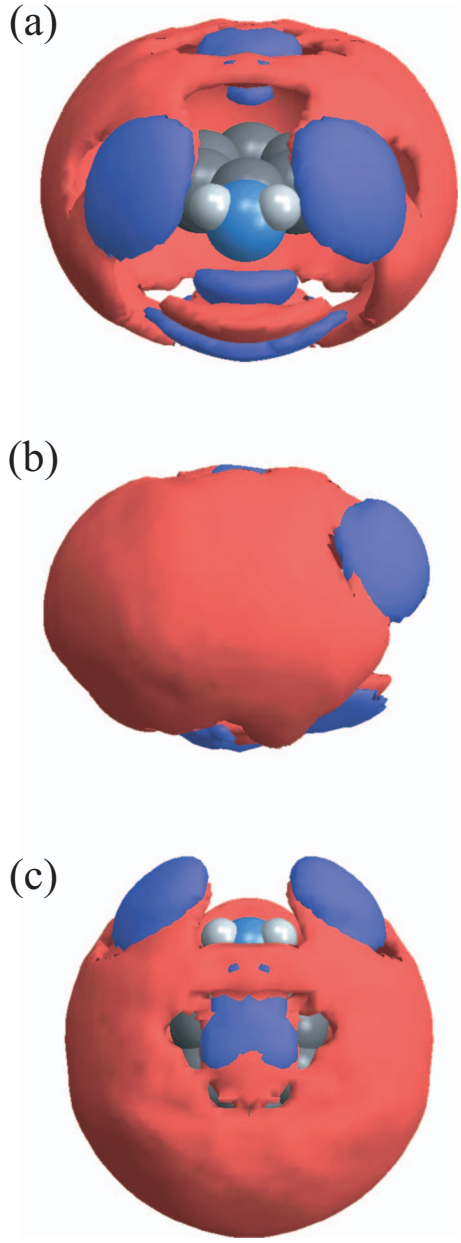

FIG. 2. (Color) The SDF of water around central aniline molecule at 298 K. Local atomic densities of oxygen (red) and hydrogen (blue) of water are shown at probability levels of $\boldsymbol{G}_O(r,\boldsymbol{\Omega})=1.65$ for oxygen and $\boldsymbol{G}_H(r,\boldsymbol{\Omega})=1.55$ for hydrogen atoms of water, respectively. (a) Front view; (b) side view; and (c) top view.

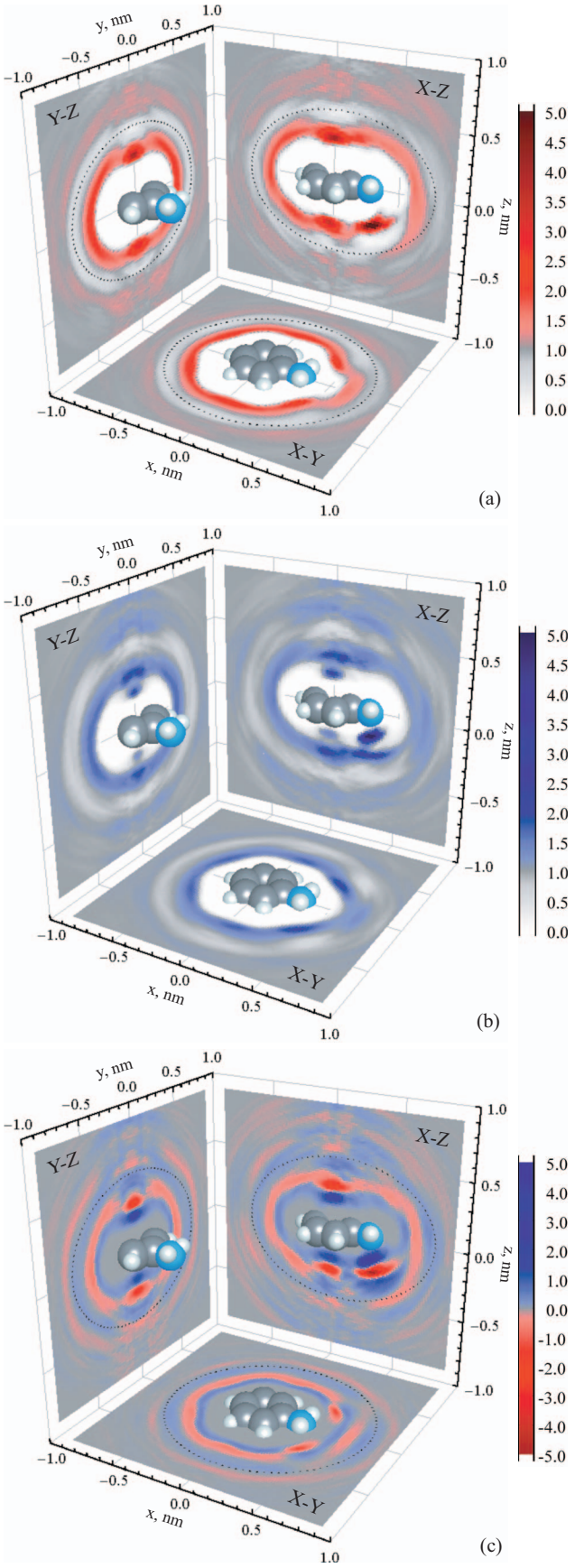

FIG. 3. (Color) 2D maps of local (a) oxygen, (b) hydrogen, and (c) charge probability densities of water around aniline at 298 K. Color depths represent probability level. The boundary of the first hydration shell is shown by the dashed line.

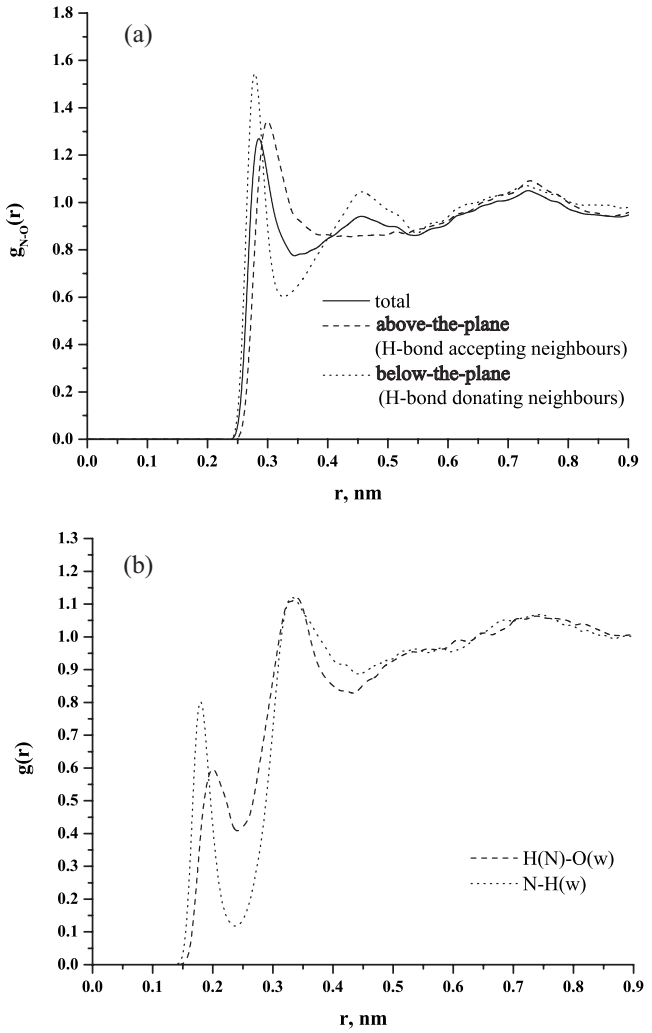

FIG. 4. Radial distribution functions between (a) nitrogen-oxygen (water) and (b) hydrogen (amino)-oxygen (water) and nitrogen-hydrogen (water) in aqueous aniline solution at 298 K.

The rigid point charge interaction potential for aniline was taken from the work of Rizzo and Jorgensen.[29] This classical OPLS-AA force field potential, optimized to reproduce experimental data for pure liquids as well as the *ab initio* hydrogen-bond strengths, was shown to yield excellent agreement with experimental results for the hydration-free energy of selected amines.[29] The geometry, charges, and Lennard-Jones (LJ) parameters are given in Table I.

MD simulations were carried out in the *NVT* ensemble along the liquid side of the coexistence curve of the SPC/E water at 298, 373, 473, and 573 with the corresponding densities being 1.00, 0.96, 0.87, and 0.67 g/cm^3, respectively. In the supercritical region simulations were performed at 633, 733, and 833 K with density fixed at 0.30 g/cm^3. The system size was 503 waters and 1 aniline molecule. The isokinetic equations of motion were integrated using the fourth-order Gear algorithm[42] with time step of 1 fs. Rotational equations of motion were represented using quaternions.[43] The equilibrated simulation run lengths were 500 ps. The long-range Coulomb forces were handled by means of Ewald sums in cubic periodic boundary conditions. The cutoff distance for the LJ interactions was set at half of

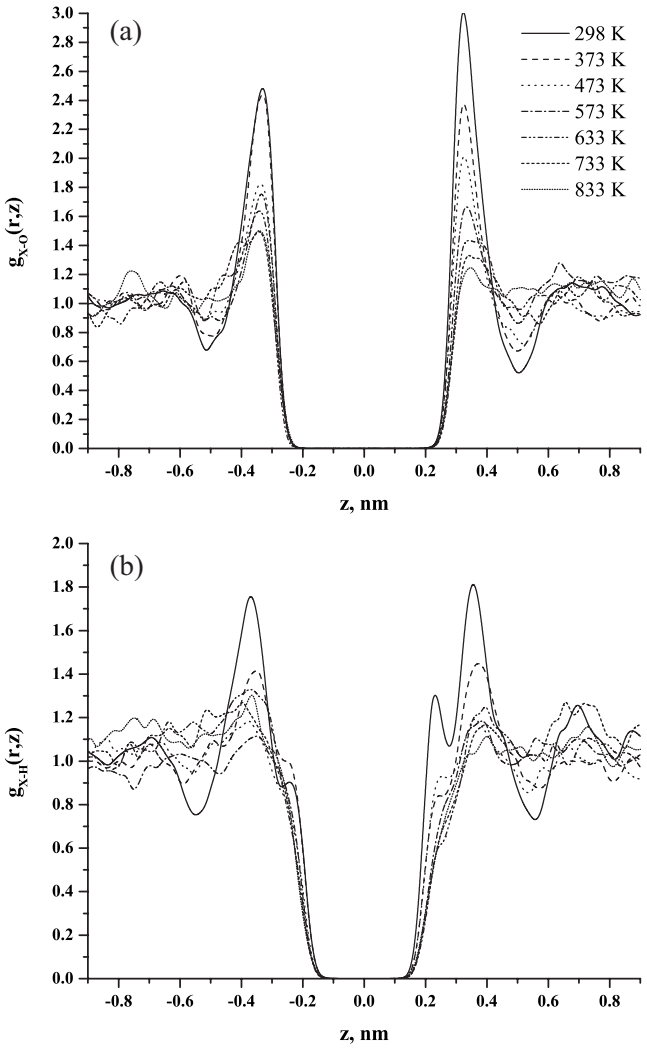

FIG. 5. CDFs of (a) oxygen and (b) hydrogen atoms of water in the axial region of the benzene ring of aniline. The origin of the local frame is at the center of the benzene ring of aniline. The radius of the cylindrical sector is 1.4 Å.

the simulation cell length. The translational diffusion coefficient was calculated from the velocity autocorrelation function (VACF). The simulations were carried out on a Linux-based parallel Transport GX28 system with dual 64 bit AMD Opteron processors.

III. RESULTS AND DISCUSSION

In this study we employ the radial, cylindrical, and spatial distribution functions (SDFs) to examine the details of the hydration of aniline molecule. The SDF (Ref. 44), or $\boldsymbol{G}(r,\boldsymbol{\Omega})$, accounts for both radial r and angular components $\boldsymbol{\Omega}=(\theta,\varphi)$ of the site-site separation vector $\boldsymbol{R}$ and is best suited for characterization of complex spatially anisotropic interactions between molecular species.[18,19,32,45–49]

The primary structure of water around aniline at ambient conditions is shown in Fig. 1. The hydrating water molecules form, as expected, both H-bond donating and H-bond accepting pairs with the amino group. Two pairs of cups along the direction of the N–H bonds are due to H-bond accepting water molecules, whereas elongated features located below the nitrogen are due to H-bond donating water molecules. In addition, water tends to form a π-type complex with the aromatic region of aniline, as indicated by the presence of a pair of contours directly above and below the center of the aromatic ring, see Fig. 1. The hydration shell of aniline at lower probability levels is drawn in Fig. 2. This figure illustrates the general shape of the hydrophobic shell around aniline.

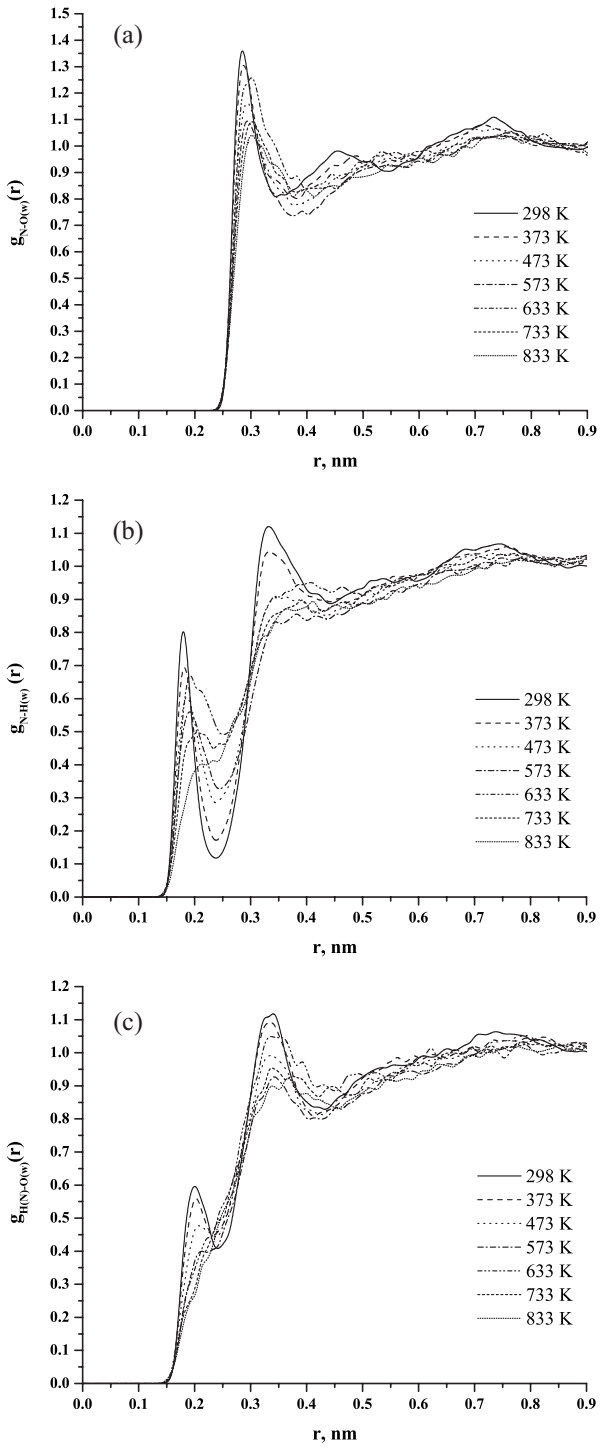

FIG. 6. Radial distribution functions between (a) nitrogen-oxygen and (b) nitrogen-hydrogen (water) and hydrogen (amino)-oxygen in aqueous aniline solution.

Details of the hydration structure of aniline can be clearly seen in Fig. 3, which displays two-dimensional (2D)

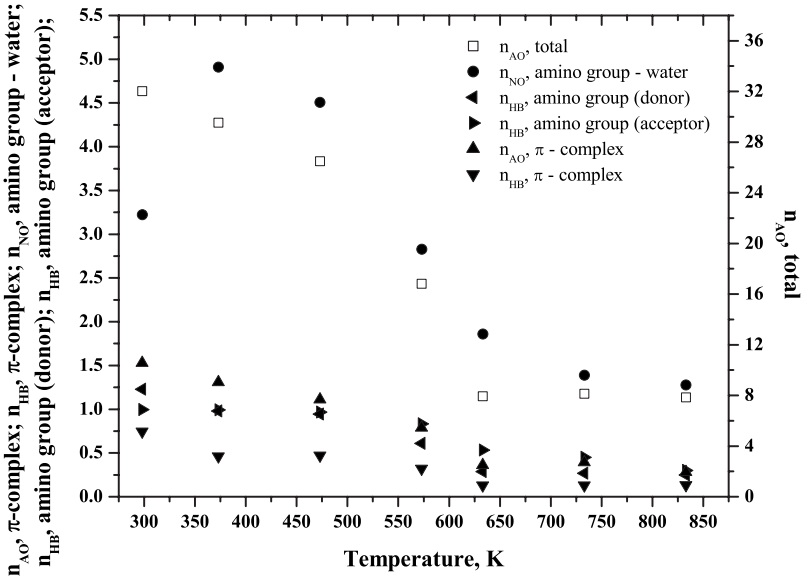

FIG. 7. Coordination numbers and number of H bonds for aniline.

density maps (cuts through the three-dimensional spatial distributions) of oxygen, hydrogen, and charge probability densities in the three orthogonal planes with respect to the symmetry of aniline molecule. The charge probability density $\boldsymbol{G}_q(r,\boldsymbol{\Omega})$ was obtained by combining the aniline-oxygen SDF $\boldsymbol{G}_{\mathrm{O}}(r,\boldsymbol{\Omega})$ and the aniline-hydrogen SDF $\boldsymbol{G}_{\mathrm{H}}(r,\boldsymbol{\Omega})$,

$$\boldsymbol{G}_{\boldsymbol{q}}(r,\boldsymbol{\Omega}) = q_{\mathrm{O}} \cdot \boldsymbol{G}_{\mathrm{O}}(r,\boldsymbol{\Omega}) + 2 \cdot q_{\mathrm{H}} \cdot \boldsymbol{G}_{\mathrm{H}}(r,\boldsymbol{\Omega}), \tag{1}$$

where q_{O} and q_{H} are the partial charges on oxygen and hydrogen atoms of water. Figure 3 clearly illustrates the most probable location and orientation of H_2N- and π-coordinated water molecules in the first hydration shell of aniline. In addition to relatively strong coordination of water molecules around the amino group and the π-region, shown with darker colors, Fig. 3 also reveals the details of the secondary, more distant features of water structure in the vicinity of the amino group. Thus, the ridge spanning around the amino group at distances from 3.5 to about 3.9 Å [see Figs. 3(a) and 3(c), *X-Z* projections] is due to the presence of a bridging water,[30] which, arguably, is H bonded to both neighbors occupying H-bond accepting sites. The charge density maps, Fig. 3(c), show details of the electrostatic environment around aniline and allow for discerning those features of the hydration structure that might not be visible on atomic density distributions. Thus, Fig. 3(c) illustrates the layered structure of the hydration shells of aniline characterized by alternating hydrogen-oxygen densities. Note that the inner and outer layers of the first hydration shell consist of primarily hydrogen atoms of water, with oxygen located in between.

The results of previous studies on methylamine indicate that the amino group is coordinated to about three water molecules with which it forms approximately two (apparently strong) hydrogen bonds. The nature of the third water molecule is somewhat unclear. Based on the analysis of the radial distribution functions (RDFs), Dunn and Nagy[25] speculated that the third "nonhydrogen bonded" water forms a bridge between the two other H-bonded neighbors. Kusalik *et al.*,[30] having examined both RDFs and SDFs, concluded that the bridging water feature, clearly resolved in the nitrogen-oxygen SDF (see Fig. 8 of Ref. 30), is located too far from the nitrogen, and therefore cannot be accounted as the extra water molecule. According to Kusalik *et al.*,[30] the nitrogen accepts a single strong H bond from water, while water, in return, accepts only one strong H bond from the amino group, where H-bond accepting water (located at the appropriate for a H-bond separation of 2.8 Å) occupies only one of the two H-bond accepting cups (see Fig. 1) at any instant in time. The second cup is occupied by a slightly more distant water molecule that is H bonded to the local hydration structure.

It should be mentioned that previous discussions in literature are based on the analysis of the nitrogen-oxygen RDF, which shows a distinct first maximum at about 2.83–2.85 Å corresponding to apparently strong N–H···O and N···H–O hydrogen bonds. The analysis of the nitrogen-oxygen SDF, obtained in this study, indicates that the maximum of the probability density for the oxygen of the H-bond donating water site is located somewhat closer to the nitrogen than that of the H-bond accepting water. In order to obtain an unambiguous picture we have used the nitrogen-oxygen SDF to compute the radial distribution function of oxygen atoms above and below the plane of the aniline molecule, Fig. 4(a). The results clearly illustrate that the total $g_{\mathrm{N-O}}(r)$ is, in fact, a combination of two different distributions. The below-the-plane $g_{\mathrm{N-O}}(r)$, which is due to the H-bond donating water, is characterized by a sharp peak located at 2.8 Å with corresponding minimum at 3.24 Å, and does indicate the presence of a strong H bond. The above-the-plane RDF (H-bond accepting neighbors) shows a broad first peak with maximum and minimum shifted to 2.98 and 4.4 Å, respectively, and therefore suggests a weaker H bond. Averaging of these two RDFs yields the first maximum at 2.83 Å with minimum at 3.42 Å, which is in agreement with the previous results.[25,30] Figure 4(b) shows a complementary set of N–H(*w*) and (N)H–O RDFs. The position and shape of the first peak in $g_{\mathrm{N-H}(w)}(r)$ with maximum and deep minimum located at 1.8 and 2.39 Å, respectively, confirm the presence of a strong H bond between the hydrogen of water

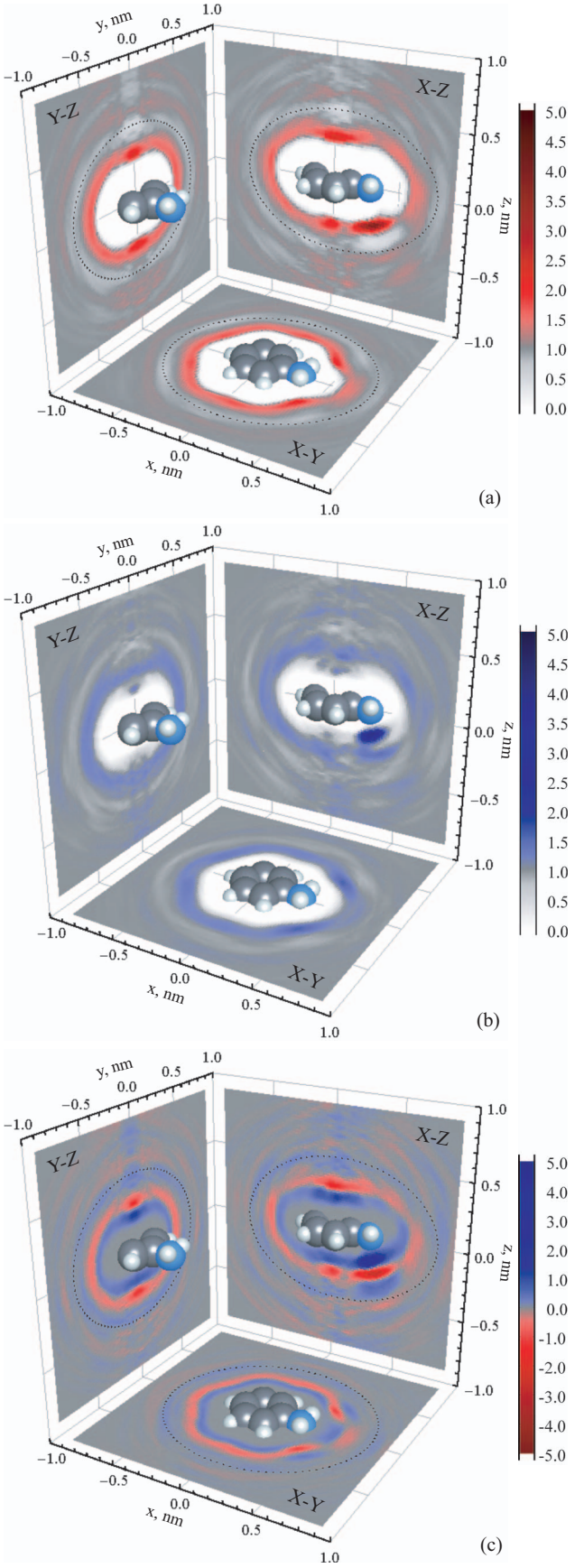

FIG. 8. (Color) 2D maps of local (a) oxygen, (b) hydrogen, and (c) charge probability densities of water around aniline at 473 K. Color depths represent probability level. The boundary of the first hydration shell is shown by the dashed line.

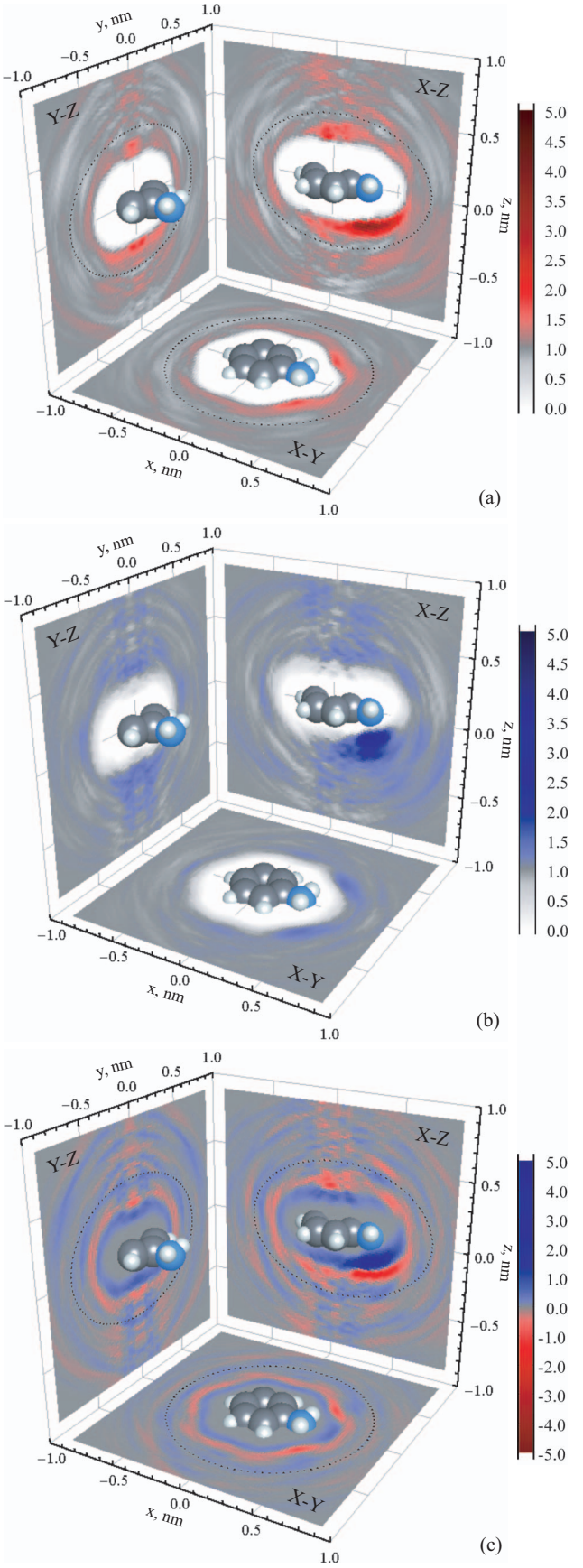

FIG. 9. (Color) 2D maps of local (a) oxygen, (b) hydrogen, and (c) charge probability densities of water around aniline at 633 K. Color depths represent probability level. The boundary of the first hydration shell is shown by the dashed line.

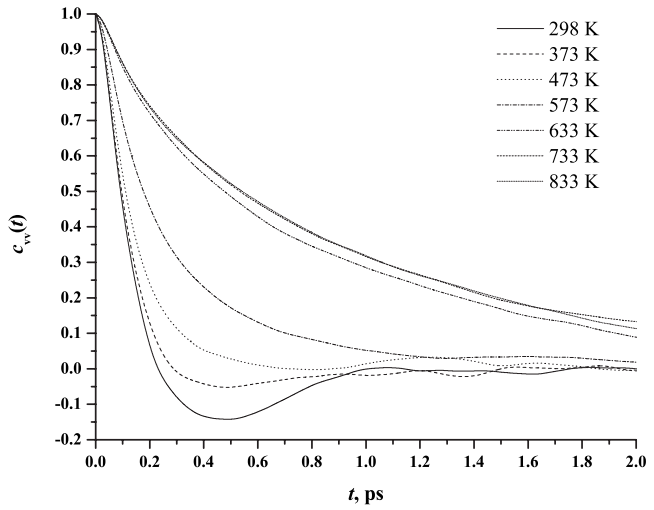

FIG. 10. Linear VACF for the center of mass of aniline in aqueous infinitely dilute solution.

and the nitrogen. Note that relative positions of the first peaks in $g_{\mathrm{N-O}}(r)$ and $g_{\mathrm{N-H}(w)}(r)$ at 2.8 and 1.8 Å, respectively, suggest a linear H bond. At the same time, the $g_{(\mathrm{N})\mathrm{H-O}}(r)$ is characterized by the first maximum at about 2.0 Å with the minimum at 2.4 Å. Thus, the H-bond accepting sites appear to be shifted farther away by about 0.2 Å from the norm for a strong H-bond location. The analysis of the coordination numbers reveals that the lone pair of nitrogen is hydrated by one water molecule with which it forms one strong linear H bond. The integration of the $g_{\mathrm{H(N)-O}}(r)$ and the above-the-plane $g_{\mathrm{N-O}}(r)$ up to 3.44 Å (actual location of the minimum is difficult to discern due to overlapping secondary structure features) indicates that each H-bond accepting cup contains close to one water molecule, forming in total two weak (0.6) H bonds with the hydrogens of the amino group. We also note that comparison of our calculated $g(r)$ results with the experimental data, once it becomes available, is clearly warranted in order to resolve any ambiguities in using this classical aniline potential.

In the analysis of coordination numbers for water molecules located in the π-region of aniline, we have employed the cylindrical distribution function (CDF) proposed by Plugatyr *et al.*[18] The CDF is well suited for characterization of the local atomic density around planar surfaces.[18,19] The CDFs of the oxygen $g_{\pi\text{-O}}(r,z)$ and hydrogen $g_{\pi\text{-H}}(r,z)$ atoms of water in aniline's aromatic region are shown in Fig. 5. Note that positive z values correspond to pair distributions above the plane of aniline, as defined in Figs. 1(a)–1(c). At 298 K, the oxygen CDF, Fig. 5(a), is characterized by the first peak located at $|z|=3.2$ Å with the corresponding minimum at $|z|=5.1$ Å. The total number of π-coordinated water molecules at ambient conditions was determined to be 1.53. The hydrogen CDF, given in Fig. 5(b), suggests the presence of weak π-type H bonds between hydrogen atoms of water and the aromatic ring, as indicated by small peaks centered at $|z|=2.3$ Å with minimum at $|z|=2.7$ Å. At 298 K the total number of π-type H bonds was determined to be 0.75. Note that the strong coordination of water molecules around the amino group of aniline affects the distribution of water molecules in the π-region, as indicated by slightly asymmetric peaks (about 10% difference in height) below and above the plane of aniline, Fig. 5.

The total coordination number of aniline was calculated from a triple integral of the aniline-oxygen SDF over the volume occupied by its hydration shell. As in our previous study,[19] the boundary of the hydration shell was determined by minimizing the average value of the $\boldsymbol{G}_{\mathrm{O}}(r,\boldsymbol{\Omega})$ on the surface of an ellipsoid. The outer boundary of the first hydration shell of aniline is shown in Fig. 3(a) by a dashed line. At ambient conditions the total coordination number of aniline was calculated to be ~32.

The changes in the primary hydration structure of aniline with temperature are illustrated in Figs. 5 and 6. As expected all peaks broaden and shift to larger distances. An apparent increase in the coordination number of the amino group at 373 and 473 K, see Fig. 7, is due to the shift in the position of the first minimum in $g_{\mathrm{N-O}}(r)$ from 3.42 Å at 298 K to 3.90 Å at 473 K. The total number of H bonds with the amino group decreases from about 1.9 at 473 K to 0.82 at 633 K and further to 0.55 at 833 K. The number of water molecules in π-coordination drops from 1.53 at ambient conditions to

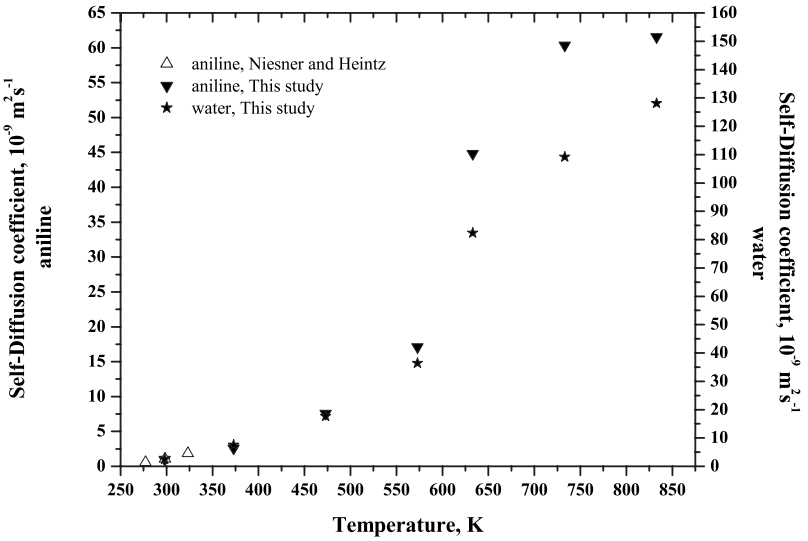

FIG. 11. Self-diffusion coefficient of aniline in aqueous infinitely dilute solution.

less than 0.3 at 833 K. The disappearance of the pronounced minima in aniline-hydrogen CDF is noted at 473 K, Fig. 5(b). The number of π-type H bonds at 473 K and above was calculated by integrating the corresponding CDF up to 2.7 Å and yielded 0.47 and 0.13 at 473 and 633, respectively. The overall coordination number of aniline decreases from 26.5 at 473 K to about eight water molecules at supercritical conditions. These changes in the hydration structure can be clearly seen in Figs. 8 and 9, which show local probability density maps at 473 and 633 K, respectively. Note an almost complete disappearance of the hydrophobic solvation shell around aniline near the critical point of water, Fig. 9.

The experimental data for the diffusivity of aniline in aqueous solution are very sparse and limited to the temperature range from 277.2 to 323.2 K.[50] In this study we employ the linear VACF to compute the self-diffusion coefficient of aniline from ambient to supercritical conditions. The length of the VACF was 4 ps. The normalized VACFs truncated at 2 ps are shown in Fig. 10. The self-diffusion coefficients of aniline along with the results for water are shown in Fig. 11. The relative uncertainty in the values for the self-diffusion for aniline in this study was estimated to be ~10%, whereas that for water is about 2%. At 298 K the self-diffusion coefficient for aniline was determined to be 0.992×10^{-9} m^2/s, which compares well with the experimental value of 1.050×10^{-9} m^2/s reported by Niesner and Heintz.[50] Note that at ambient conditions the VACF shows a pronounced minimum at about 0.5 ps, which indicates a cage effect. As expected, the self-diffusion coefficient of aniline increases with temperature. The disappearance of the characteristic minimum in the VACF of aniline is observed around 473 K, which coincides with the loss of the π-coordinated water molecules and illustrates the overall weakening of the hydration shell structure around aniline with temperature. A dramatic rise in the diffusivity of aniline is observed around 633 K. We recall that at these conditions the hydration cage around aniline essentially disappears. This observation is supported by a nearly exponential decay of the VACFs obtained at supercritical conditions, which suggest very weak intermolecular interactions. We also note a rather weak temperature dependence of the self-diffusion coefficient of aniline along the critical isochore above the critical point (at 733 and 833 K). Similar behavior of the self-diffusion coefficients of hydrophobic solutes in the medium density supercritical water has been reported by Ohmori and Kimura[16] and observed in our previous studies.[18,19]

IV. CONCLUSIONS

MD simulations of aqueous aniline at infinite dilution were carried out along the liquid branch of the coexistence curve of water as well as in the supercritical region. The spatial structure of water around the aniline molecule was calculated and analyzed in detail. It is shown that the hydration shell of aniline in the supercritical region differs dramatically from that at ambient conditions. At room temperature a well defined solvent shell of aniline is comprised of ~32 water molecules, three of which are coordinated to the amino group by donating one strong (lone pair site) and accepting two weak (0.6) H bonds. The results also indicate the formation of weak π-complexes between hydrogen of water and the aromatic ring of aniline. Thus, at ambient conditions 1.5 water molecules were identified as π-coordinated, forming close to 0.75 π-H bonds. The analysis of the results obtained at elevated temperatures indicates that the hydration shell around aniline begins disappearing at around 473 K at saturation, which is reflected in the loss of π-coordinated water, and virtually disappears near the critical point of water. At 633 K and 0.3 g/cm^3 aniline is solvated by only eight water molecules and forms close to one H bond in total. The changes in the hydration structure with temperature (and density) are reflected in the value of the self-diffusion coefficient of aniline, which shows a dramatic rise near the critical point of water. Based on the obtained results, we may speculate that the apparent decrease in rate constants for reactions of substituted benzenes with OH radicals in aqueous solution at subcritical conditions (see Refs. 7, 8, 11, and 15) is arguably due to the lack of stabilization of the reactive π-complexes by the hydrating water molecules.

ACKNOWLEDGMENTS

We express our gratitude to the Natural Sciences and Engineering Research Council of Canada for financial support.

[1] M. D. Bermejo and M. J. Cocero, AIChE J. **52**, 3933 (2006).
[2] A. Kruse and E. Dinjus, J. Supercrit. Fluids **39**, 362 (2007).
[3] A. Kruse and E. Dinjus, J. Supercrit. Fluids **41**, 361 (2007).
[4] A. Kruse and H. Vogel, Chem. Eng. Technol. **31**, 1241 (2008).
[5] Ph. MacDonald, J. Buongiorno, J. W. Sterbentz, C. Davis, and R. Witt, "Feasibility study of supercritical light water cooled reactors for electric power production," Nuclear Energy Research Initiative Project 2001-001 Report No. INEEL/EXT-04-02530.
[6] J. Kronholm, K. Hartonen, and M.-L. Riekkola, TrAC, Trends Anal. Chem. **26**, 396 (2007).
[7] L. Ashton, G. V. Buxton, and C. R. Stuart, J. Chem. Soc., Faraday Trans. **91**, 1631 (1995).
[8] J. Feng, S. N. V. K. Aki, J. E. Chateauneuf, and J. F. Brennecke, J. Am. Chem. Soc. **124**, 6304 (2002).
[9] K. Takahashi, D. M. Bartels, J. A. Cline, and C. D. Jonah, Chem. Phys. Lett. **357**, 358 (2002).
[10] J. Cline, K. Takahashi, T. W. Marin, C. D. Jonah, and D. M. Bartels, J. Phys. Chem. A **106**, 12260 (2002).
[11] T. W. Marin, J. A. Cline, K. Takahashi, D. M. Bartels, and C. D. Jonah, J. Phys. Chem. A **106**, 12270 (2002).
[12] K. Ghandi, B. Addison-Jones, J. C. Brodovitch, I. McKenzie, P. W. Percival, and J. Schuth, Phys. Chem. Chem. Phys. **4**, 586 (2002).
[13] K. Ghandi and P. W. Percival, J. Phys. Chem. A **107**, 3005 (2003).
[14] I. Janik, D. M. Bartels, and C. D. Jonah, J. Phys. Chem. A **111**, 1835 (2007).
[15] J. Bonin, I. Janik, D. Janik, and D. M. Bartels, J. Phys. Chem. A **111**, 1869 (2007).
[16] T. Ohmori and Y. Kimura, J. Chem. Phys. **119**, 7328 (2003).
[17] C. Nieto-Draghi, J. B. Avalos, O. Contreras, P. Ungerer, and J. Ridard, J. Chem. Phys. **121**, 10566 (2004).
[18] A. Plugatyr, I. Nahtigal, and I. M. Svishchev, J. Chem. Phys. **124**, 024507 (2006).
[19] I. M. Svishchev, A. Plugatyr, and I. G. Nahtigal, J. Chem. Phys. **128**, 124514 (2008).
[20] W. J. Lamb, G. A. Hoffman, and J. Jonas, J. Chem. Phys. **74**, 6875 (1981).
[21] K. Yoshida, C. Wakai, N. Matubayasi, and M. Nakahara, J. Chem. Phys. **123**, 164506 (2005).
[22] U. Spoerel and W. Stahl, J. Mol. Spectrosc. **190**, 278 (1998).
[23] Y. Inokuchi, K. Ohashi, Y. Honkawa, N. Yamamoto, H. Sekiya, and N. Nishi, J. Phys. Chem. A **107**, 4230 (2003).

[24] G. Piani, M. Pasquini, I. Lopez-Tocon, G. Pietraperzia, M. Becucci, and E. Castellucci, Chem. Phys. **330**, 138 (2006).
[25] W. J. Dunn and P. I. Nagy, J. Phys. Chem. **94**, 2099 (1990).
[26] W. J. Dunn, P. I. Nagy, and E. R. Collantes, J. Am. Chem. Soc. **113**, 7898 (1991).
[27] E. C. Meng, J. W. Caldwell, and P. A. Kollman, J. Phys. Chem. **100**, 2367 (1996).
[28] M. M. Kubo, E. Gallicchio, and R. M. Levy, J. Phys. Chem. B **101**, 10527 (1997).
[29] R. C. Rizzo and W. L. Jorgensen, J. Am. Chem. Soc. **121**, 4827 (1999).
[30] P. G. Kusalik, D. Bergman, and A. Laaksonen, J. Chem. Phys. **113**, 8036 (2000).
[31] A. V. Gubskaya and P. G. Kusalik, J. Phys. Chem. A **108**, 7165 (2004).
[32] P. Jedlovszky and A. Idrissi, J. Chem. Phys. **129**, 164501 (2008).
[33] H. J. C. Berendsen, J. R. Grigera, and T. P. Straatsma, J. Phys. Chem. **91**, 6269 (1987).
[34] Y. Guissani and B. Guillot, J. Chem. Phys. **98**, 8221 (1993).
[35] M. Neumann, Proceedings of the 12th International Conference on the Properties of Water and Steam, 1995 (unpublished), pp. 261–268.
[36] A. A. Chialvo and P. T. Cummings, J. Phys. Chem. **100**, 1309 (1996).
[37] J. R. Errington, K. Kiyohara, K. E. Gubbins, and A. Z. Panagiotopoulos, Fluid Phase Equilib. **150–151**, 33 (1998).
[38] G. C. Boulougouris, I. G. Economou, and D. N. Theodorou, J. Phys. Chem. B **102**, 1029 (1998).
[39] T. M. Hayward and I. M. Svishchev, Fluid Phase Equilib. **182**, 65 (2001).
[40] J. Alejandre, D. J. Tildesley, and G. A. Chapela, J. Chem. Phys. **102**, 4574 (1995).
[41] J. R. Errington and A. Z. Panagiotopoulos, J. Phys. Chem. B **102**, 7470 (1998).
[42] D. J. Evans and O. P. Morriss, Comput. Phys. Rep. **1**, 297 (1984).
[43] D. J. Evans, Mol. Phys. **34**, 317 (1977).
[44] P. G. Kusalik and I. M. Svishchev, Science **265**, 1219 (1994).
[45] A. Laaksonen, P. Stilbs, and R. E. Wasylishen, J. Chem. Phys. **108**, 455 (1998).
[46] K. S. Sidhu, J. M. Goodfellow, and J. Z. Turner, J. Chem. Phys. **110**, 7943 (1999).
[47] P. G. Kusalik, A. P. Lyubartsev, D. L. Bergman, and A. Laaksonen, J. Phys. Chem. B **104**, 9526 (2000).
[48] T. M. Raschke and M. Levitt, J. Phys. Chem. B **108**, 13492 (2004).
[49] D. T. Bowron, J. L. Finney, and A. K. Soper, J. Phys. Chem. B **110**, 20235 (2006).
[50] R. Niesner and A. Heintz, J. Chem. Eng. Data **45**, 1121 (2000).